

## NATURE OF THE ILLITIC PHASE ASSOCIATED WITH RANDOMLY INTERSTRATIFIED SMECTITE/ILLITE IN SOILS\*

D. A. LAIRD<sup>1</sup> AND E. A. NATER<sup>2</sup>

<sup>1</sup> D. A. Laird, USDA-ARS, National Soil Tilth Laboratory  
2150 Pammel Drive, Ames, Iowa 50011

<sup>2</sup> E. A. Nater, Department of Soil Science, University of Minnesota  
1991 Upper Buford Circle, St. Paul, Minnesota 55108

**Abstract**—A dispersion-centrifugation-decantation procedure was used to isolate various particle size fractions from a sample of clay (<2  $\mu\text{m}$  fraction) separated by sedimentation from the Ap horizon of a Webster soil (fine-loamy, mixed, mesic Typic Haplaquoll). The 0.02–0.06  $\mu\text{m}$  size fraction was found to be enriched in an illitic phase associated with randomly interstratified smectite/illite. X-ray powder diffraction, chemical analysis, and high-resolution transmission electron microscopy confirmed that most of the illitic material in the 0.02–0.06  $\mu\text{m}$  size fraction was composed of two-layer elementary illite particles with a layer charge of  $-0.47$  per formula unit. The results demonstrate that this low-charge illitic phase can be physically separated from soil materials and that the low-charge illitic phase has chemical, morphological, and mineralogical properties that are uniquely different from those of smectite and illite.

**Key Words**—Chemical analysis, Elementary particle, High-resolution transmission electron microscopy, Illite, Interstratified, Smectite, Smectite/illite.

### INTRODUCTION

In a recent study, Laird *et al.* (1991a) determined the elemental compositions of the illitic and smectitic phases in randomly interstratified smectite/illite from a typical agricultural soil. To do so, six fine clay fractions (<0.020, <0.026, <0.036, <0.045, <0.060, and <0.090  $\mu\text{m}$ ) were separated from a soil clay sample (<2.0  $\mu\text{m}$  size fraction). They were then saturated with Ca, washed free of excess electrolytes, and analyzed for nine elements by inductively coupled plasma-atomic emission spectroscopy (ICP-AES) using suspension nebulization. Based on results from X-ray powder diffraction (XRD) and chemical analyses, it was hypothesized that the fine clay samples contained various proportions of only two mineral phases, a K-bearing “illitic phase” and a K-free “smectitic phase.” To facilitate interpretation of the chemical analysis, a nonlinear elemental mass balance model was developed. Three assumptions were needed for the model: 1) that only two mineral phases were present in the various fine clay samples; 2) that the average elemental composition of both mineral phases was the same in all of the fine clay samples; and 3) that all of the K in the fine clay samples was associated with the illitic phase. The first two assumptions were supported by the linearity of the K vs other element relationships and by XRD

analysis of the fine clay samples. The third assumption is fundamental to the concept of smectite and illite. Parameters for the nonlinear elemental mass balance model were optimized using the Marquardt algorithm (Bevington, 1969) as modified by Barak *et al.* (1990) and independently verified by water mass balance.

The smectitic phase identified in the work of Laird *et al.* (1991a) is a high-charge ( $-0.482$  per formula unit), Fe-rich montmorillonite with 46.6% tetrahedral charge. The illitic phase is a dioctahedral, tetrahedrally charged (86.9% tetrahedral charge) 2:1 phyllosilicate with a total layer charge of  $-0.473$  per formula unit. The illitic phase has a K to Ca equivalent ratio of 1:1, from which we inferred that the illitic phase is composed of two-layer elementary illite particles (Nadeau *et al.*, 1984a, 1984b) structurally similar to rectorite. Such elementary illite particles consist of two 2:1 phyllosilicate layers coordinated by dehydrated interlayer K, with hydrated cations (e.g., Ca) satisfying the permanent charge on the external surfaces of the elementary particles.

This study was initiated to test the prediction of Laird *et al.* (1991a) that a major portion (over 22% w/w) of the Webster soil clay (<2  $\mu\text{m}$  fraction) consists of two-layer, low-charge, elementary illite particles. The specific objectives of the study were 1) to isolate a soil clay fraction that is substantially enriched in the illitic phase associated with randomly interstratified smectite/illite and 2) to characterize the chemistry, morphology, and mineralogy of the illitic phase in that fraction.

\* Joint contribution of the USDA-ARS and the Minnesota Agricultural Experimental Station. Paper 19,786 of the Scientific Journal Series.

## MATERIALS AND METHODS

The soil sample used in this study was collected from the Ap horizon of a Webster (fine-loamy, mixed, mesic Typic Haplaquoll, pedon located on the University of Minnesota Southern Agricultural Experiment Station, near Waseca, Minnesota. A portion (1 kg) of the soil sample was dispersed in distilled water by mechanical agitation and fractionated by sedimentation to separate a bulk clay (<2  $\mu\text{m}$  size fraction) sample. The clay sample was air-dried and crushed in an agate mortar. The same bulk soil clay sample was used in Laird *et al.* (1991a).

A portion of the bulk soil clay was sequentially fractionated to produce samples of the <0.02, 0.02–0.06, 0.06–0.09, 0.09–0.18, 0.18–0.36, and 0.36–2.0  $\mu\text{m}$  size fractions. To do so, organic matter and sesquioxides were removed from the soil clay by treatment with 30%  $\text{H}_2\text{O}_2$  and dithionite-citrate-bicarbonate (DCB), respectively (Kunze and Dixon, 1986). Six samples (0.75 g each) of the  $\text{H}_2\text{O}_2$ -DCB-treated clay were washed two times with 25 ml of 2 M NaCl and once with 25 ml of distilled water. These samples were dispersed in 25 ml of distilled water by a combination of mechanical agitation and sonication (30 s at 40 W) treatments, centrifuged at the appropriate speed (Jackson, 1985), and decanted. The dispersion-centrifugation-decantation procedure was repeated four times for each fractionation step. The various separates were combined to produce one sample of each of the indicated size fractions. The samples were flocculated with  $\text{CaCl}_2$ , washed 3 times with 0.5 M  $\text{CaCl}_2$ , washed 8 times with 95% ethanol, air-dried, and then crushed in an agate mortar. The entire procedure was repeated to produce replicate samples of the six size fractions.

Portions of the Ca-saturated 0.02–0.06  $\mu\text{m}$  size fraction were washed three times with either 0.5 M  $\text{MgCl}_2$  or 1 M KCl, and then washed 4 times with 95% ethanol to produce Mg- and K-saturated samples, respectively. The various Ca-, Mg-, and K-saturated samples were oriented on glass slides by the paste method (Theissen and Harward, 1962), air-dried (~50% relative humidity), and analyzed by XRD. The Mg-saturated sample was solvated with glycerol by slurring the clay with 10% (v/v) glycerol-90% ethanol, and then reanalyzed by XRD. The K-saturated sample was analyzed a second time by XRD after a 2 hr 105°C heat treatment and a third time after rewetting with a few drops of distilled water.

A portion (0.1 g) of the 0.02–0.06  $\mu\text{m}$  size fraction was washed once with 5 ml of 0.065 M octadecylamine hydrochloride and then incubated with a fresh 5 ml aliquot of 0.065 M octadecylamine hydrochloride at 60°C for 3 hr. Following incubation, the sample was washed 4 times with 20 ml of 95% ethanol. A portion of the octadecylammonium-treated clay (C18-clay) was prepared as an oriented specimen on a glass slide for

XRD analysis. Another portion of the C18-clay was slurried with Quetol<sup>1</sup> resin, spread uniformly as a thin film over a flat Teflon surface, and cured for 24 hr at 60°C. Fresh resin was added on top of the cured resin-C18-clay film and cured for an additional 24 hr at 60°C to produce a block of cured resin with the C18-clay concentrated in a thin layer on a flat surface of the block (Laird *et al.*, 1989). A second block of resin was prepared in a similar manner but without clay for use as a blank. Both resin blocks and the oriented C18-clay specimen were analyzed by XRD. All XRD analyses were performed using  $\text{CuK}\alpha$  radiation and a Philips APD 3720 X-ray diffractometer equipped with a focusing graphite monochromator.

Thin sections of the resin block containing the C18-clay were cut with an ultra-microtome using a diamond knife. The thin sections were cut perpendicular to the orientation of the C18-clay film within the block, mounted on 1000-mesh Cu grids, carbon coated, and analyzed by high-resolution transmission electron microscopy (HRTEM). The HRTEM analysis was performed with a Philips CM30 Transmission Electron Microscope operated at 300 kV. The specimen stage was cooled with liquid nitrogen.

Elemental analyses of the Ca-saturated, 0.02–0.06  $\mu\text{m}$  size fraction and the C18-clay were performed by ICP-AES using suspension nebulization (Laird *et al.*, 1991b). To do so, 0.05 g of air-dry clay were sonicated for 10 min at 80 W in 50 ml of 0.1 M NaCl. The chemical analysis was performed with an Applied Research Laboratories (ARL) Model 3560 inductively coupled plasma-atomic emission spectrometer. A peristaltic pump was used with an ARL Maximum Dissolved Solids nebulizer and a conical spray chamber to provide a uniform nebulization rate of 2.6 ml min<sup>-1</sup>. Incident power was 1200 W, observation height was 15 mm above the top load coil, and carrier Ar pressure was 1.59 mPa. The spectrometer was calibrated with multielement solution standards prepared with 0.1 M NaCl matrix solutions, and all samples and standards contained a 10 mg liter<sup>-1</sup> Co internal standard.

## RESULTS AND DISCUSSION

X-ray powder diffraction patterns are presented in Figure 1 for various particle size fractions of the Webster soil clay. Percentages (w/w) of each size fraction in the whole soil clay are also presented in Figure 1. The percentages are based on average gravimetric recoveries for replicate separations of each size fraction and have been normalized to sum to 100%. Total re-

<sup>1</sup> Trade names and company names are included for the benefit of the reader and do not imply any endorsement of the product by the USDA or the Minnesota Agricultural Experimental Station.

covery (sum of recoveries for all size fractions) was 82% of the starting weight.

The XRD patterns in Figure 1 illustrate the relationship between mineralogy and particle size for the Webster soil clay. Quartz (4.26 and 3.34 Å XRD peaks) is the dominant mineral phase in the coarsest clay fraction (0.36–2.0 μm size fraction) but is largely absent in finer fractions. Faint alkali feldspar (3.79 and 3.25 Å) and plagioclase (4.04 and 3.21 Å) peaks are also present in the XRD pattern for the 0.36–2.0 μm size fraction. The feldspar peaks are difficult to distinguish from background in the XRD pattern of the whole clay (<2 μm) and cannot be distinguished in the XRD patterns for any clay fractions finer than 0.36 μm. Distinct kaolinite (7.2 and 3.56 Å) peaks are evident in the XRD patterns for the 0.36–2.0, 0.18–0.36, 0.09–0.18, and 0.06–0.09 μm size fractions and are difficult to distinguish in the XRD patterns for the 0.02–0.06 and <0.02 μm size fractions. Smectite is overwhelmingly concentrated in the finest clay fraction as evidenced by the broad 14 Å peak in the XRD pattern for the <0.02 μm size fraction. The nature of the illitic material in the Webster soil clay varies systematically with size fraction. A distinct 10.0 Å peak is evident in the XRD pattern for the 0.36–2.0 μm size fraction (Figure 1), indicating the presence of discrete multilayered illite particles in the coarse clay. By contrast, there is a low-intensity plateau stretching from 10.0 to 14 Å in the XRD pattern for the 0.18–0.36 μm size fraction that progressively shifts towards lower angles with decreasing particle size until it forms a broad low-intensity peak centered on 14 Å in the XRD pattern for the 0.02–0.06 μm size fraction. This shift indicates increasing disorder in the illitic materials with decreasing size fraction.

The K content of the 0.02–0.06 μm size fraction ( $K = 18.09 \text{ g kg}^{-1}$ ) indicates that the sample contains a substantial amount of "illitic" material. Following standard convention (e.g., % illite = %  $K_2O \times 10$ ; Jackson *et al.*, 1986), one estimates 22% (w/w) illite in the 0.02–0.06 μm size fraction. The standard convention, however, is based on the assumption that illite has a layer charge of 0.8 per formula unit and that all permanent charge sites in illite are satisfied by K. Such high-charged, multilayered, illite particles ought to yield a 10.0 Å XRD peak; however, the XRD pattern for the 0.02–0.06 μm size fraction (Figure 1) does not exhibit a distinct 10.0 Å peak. On the other hand, elementary illite particles do not yield 10.0 Å XRD peaks because they have too few contiguous layers with 10.0 Å spacings for coherent diffraction of X-radiation. Therefore, the fact that the 0.02–0.06 μm size fraction contains 18.09 g  $\text{kg}^{-1}$  K yet does not exhibit a 10.0 Å XRD peak suggests that the illitic material in the sample is composed primarily of elementary illite particles. Indeed, the relationship (% illitic phase = %  $K_2O \times 34.4$ ; note that units are different in the original source)

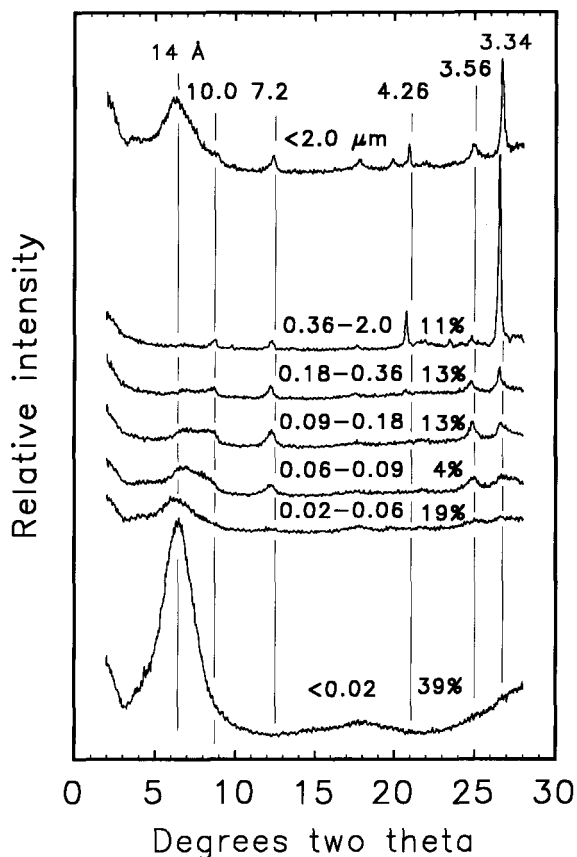


Figure 1. X-ray powder diffraction patterns of the <2 μm size fraction and various fractions separated from the <2 μm size fraction of the Ap horizon of a Webster soil. Normalized percent recoveries for fractions separated from the <2 μm size fraction are given above the XRD patterns. The samples were Ca-saturated, air-dried, and analyzed with  $\text{CuK}\alpha$  radiation.

presented by Laird *et al.* (1991a) for the same materials indicates that 75% (w/w) of the 0.02–0.06 μm size fraction is composed of elementary illite particles.

Small portions of the 0.02–0.06 μm size fraction were saturated with Mg and K and analyzed by XRD (Figure 2). The Mg-saturated, air-dried sample (A in Figure 2) exhibits a broad 14 Å XRD peak and higher order reflections near 4.9 and 3.4 Å. After glycerol solvation (B in Figure 2), the 14 Å peak expanded to 18 Å with broad 9, 4.7, and 3.5 Å higher order reflections. Similar peak positions were reported by Reynolds (1980) for calculated XRD patterns of glycolated, randomly interstratified, 60/40 smectite/illite (note that a 60/40 S/I in the nomenclature used by Reynolds contains 20% elementary smectite particles and 80% elementary illite particles). The K-saturated, air-dried sample has a prominent 10.0 Å XRD peak with higher order reflections at 4.92 and 3.33 Å (C in Figure 2). No change is apparent in the XRD pattern of the K-saturated sample after a 2 hr 105°C heat treatment (D in Figure 2);

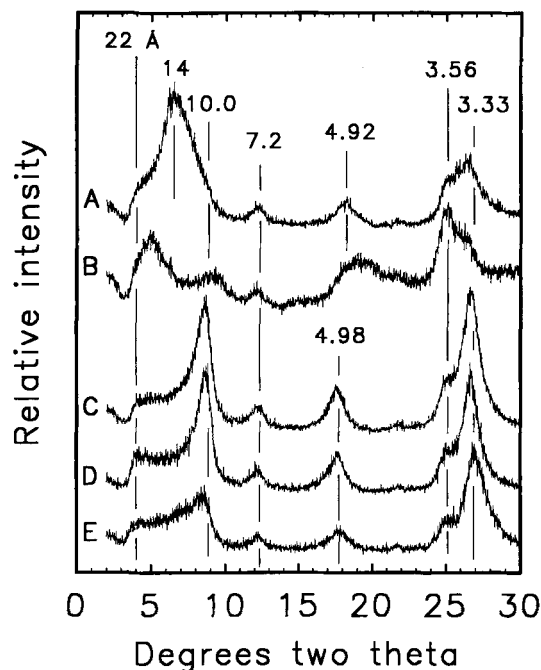


Figure 2. X-ray powder diffraction patterns of the 0.02–0.06  $\mu\text{m}$  size fraction separated from the Ap horizon of the Webster soil. Treatments include: A) Mg-saturated and air-dried ( $\sim 50\%$  relative humidity), B) Mg-saturated and glycerol solvated, C) K-saturated and air-dried ( $\sim 50\%$  relative humidity), D) K-saturated and oven-dried ( $105^\circ\text{C}$  2 hr), and E) K-saturated, oven-dried, and rewet. The samples were analyzed with  $\text{CuK}\alpha$  radiation.

however, the intensity of the 10.0 Å XRD peak decreased when the sample was rewet (E in Figure 2). A low-angle shoulder stretching to 22 Å is evident in all of the XRD patterns for the K-saturated sample. The low-angle shoulder is probably a superlattice reflection for sets of contiguous elementary illite particles.

Results for chemical analysis of the Ca-saturated 0.02–0.06  $\mu\text{m}$  size fraction are presented in Table 1 along with elemental concentrations for this fraction as predicted from the measured K content of the sample and the K vs other element regression equations presented by Laird *et al.* (1991a). There is very good agreement between the measured and predicted elemental concentrations in Table 1 for all major elements, despite the fact that the K content ( $18.09 \text{ g kg}^{-1}$ ) of the 0.02–0.06  $\mu\text{m}$  size fraction is substantially out-

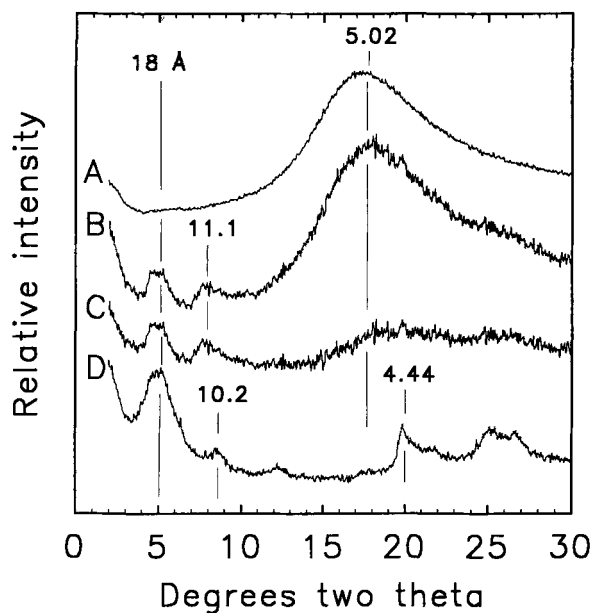


Figure 3. X-ray powder diffraction patterns for a block of Quetol resin (A), the C18-treated 0.02–0.06  $\mu\text{m}$  size fraction of the Webster soil in a block of Quetol resin (B), and the C18-treated 0.02–0.06  $\mu\text{m}$  size fraction of the Webster soil oriented on a glass slide (D). (C) is a differential XRD pattern showing the C18-treated 0.02–0.06  $\mu\text{m}$  size fraction of the Webster soil in Quetol resin without the resin effect (obtained by subtracting pattern B from pattern A). The samples were analyzed with  $\text{CuK}\alpha$  radiation.

side of the K range ( $4.4\text{--}9.2 \text{ g kg}^{-1}$ ) for the samples used in the original regression analysis. Theoretically, mixtures containing various proportions of two mineral phases will yield linear K vs other element relationships, where mixtures of three (or more) phases will yield nonlinear relationships unless quantities of two of the phases vary in exact proportion to each other. Such proportional variation is unlikely, as illustrated by the relationships between particle size and mineralogy in Figure 1. Therefore, the agreement between the measured and predicted elemental concentrations in Table 1 supports the assumption of Laird *et al.* (1991a) that the fine clay fractions ( $<0.09 \mu\text{m}$ ) of the Webster soil clay consist of mixtures of only two phases. The small kaolinite XRD peaks (7.2 and 3.56 Å) evident in Figure 2, however, demonstrate that the assumption is not entirely valid.

Table 1. Measured and predicted elemental compositions of the 0.02–0.06  $\mu\text{m}$  size fraction separated from the Ap horizon of a Webster soil. Measured K concentration was  $18.09 \text{ g kg}^{-1}$ .

	$\text{g kg}^{-1}$							
	Si	Al	Fe	Ca	Mg	Mn	Zn	Ti
Measured	279.0	130.4	56.02	16.58	14.95	0.255	0.317	3.556
Predicted	279.6	130.9	54.01	16.79	15.04	0.211	0.259	3.955
% Error	+0.2	+0.4	-3.6	+1.2	+0.6	-17	-18	+11

Table 2. Structural formulas for the illitic phase associated with randomly interstratified smectite/illite in soils. The formulas were calculated from the data of Laird *et al.* (1991a) after deducting elemental contributions due to 0, 2.5, and 5% kaolinite contamination.

Assumed percent kaolinite	Cations per formula unit [O <sub>10</sub> (OH) <sub>2</sub> ]									
	Interlayer		Tetrahedral				Octahedral			
	Ca <sup>2+</sup>	K <sup>+</sup>	Si <sup>4+</sup>	Al <sup>3+</sup>	Al <sup>3+</sup>	Fe <sup>3+</sup>	Mg <sup>2+</sup>	Mn <sup>2+</sup>	Zn <sup>2+</sup>	Ti <sup>4+</sup>
0	0.120	0.233	3.589	0.411	1.514	0.259	0.230	0.001	0.001	0.039
2.5	0.123	0.240	3.601	0.399	1.492	0.266	0.237	0.001	0.001	0.040
5	0.125	0.246	3.613	0.387	1.471	0.273	0.243	0.002	0.001	0.041

The effect of kaolinite contamination in the fine clay fractions of the Webster soil clay on the calculated structural formula for the illitic phase in the randomly interstratified smectite/illite is minimal. To demonstrate this point, the structural formula for the illitic phase was recalculated using the chemical composition of the illitic phase as determined by Laird *et al.* (1991a), but after subtracting elemental contributions for 0, 2.5, and 5% kaolinite (Table 2). Even if kaolinite contamination were as high as 5%, the calculated layer charge of the illitic phase only increases from  $-0.473$  to  $-0.496$  per formula unit, the K:Ca equivalent ratio increases from 0.97 to 0.98, and the percent tetrahedral charge decreases from 87% to 78%.

A portion of the 0.02–0.06  $\mu\text{m}$  size fraction was treated with octadecylamine hydrochloride, embedded in epoxy resin, and analyzed by both XRD and HRTEM. Alkylammonium cations have been shown to displace K from micaceous minerals (Laird *et al.*, 1987; Mackintosh and Lewis, 1968). Therefore, to avoid damaging the illitic material in the 0.02–0.06  $\mu\text{m}$  size fraction, a relatively mild alkylammonium treatment was used in preparing the C18-clay. After treatment, the C18-clay contained nearly as much K as the Ca-saturated sample (17.99 and 18.09  $\text{g kg}^{-1}$  K in the C18-treated and Ca-saturated samples, respectively), indicating that the C18-treatment did not cause significant K-depletion of the 0.02–0.06  $\mu\text{m}$  size fraction. The mild alkylam-

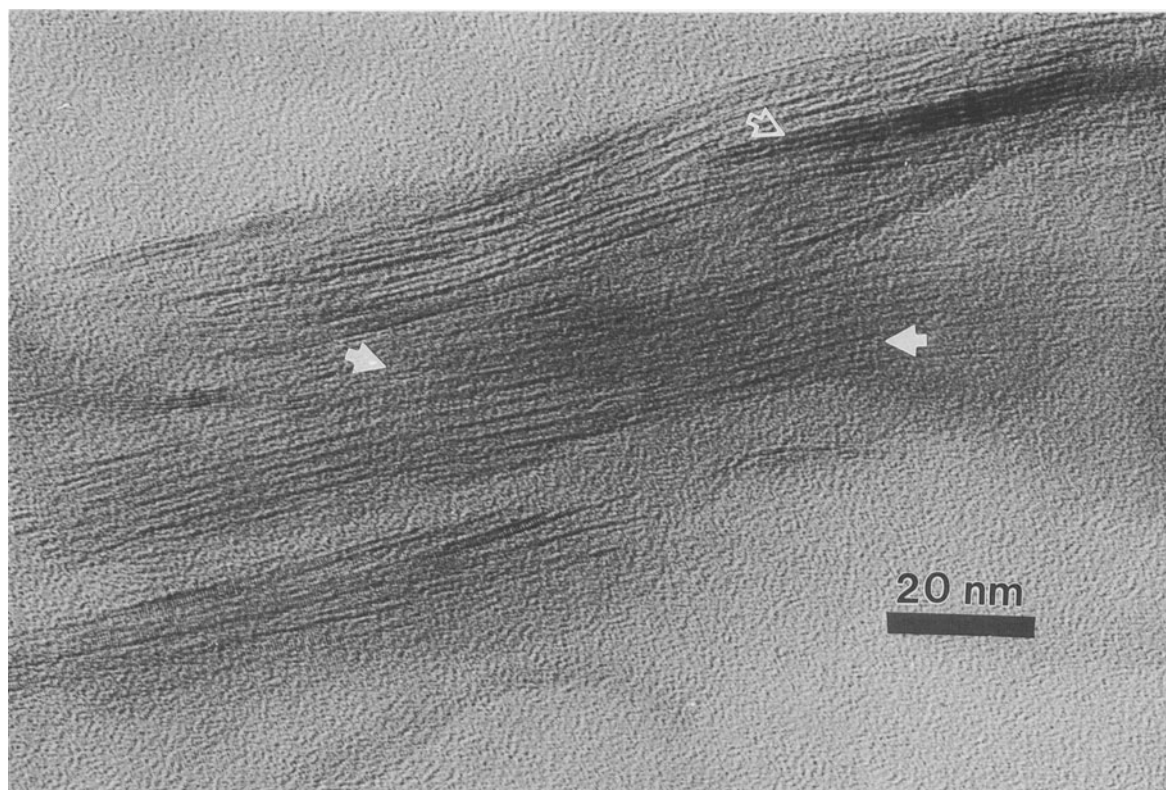


Figure 4. HRTEM lattice image of the C18-treated 0.02–0.06  $\mu\text{m}$  size fraction of the Webster soil showing two-layer elementary illite particles (solid arrows = 20.2  $\text{\AA}$ ) and multilayer illite (hollow arrow = 10  $\text{\AA}$ ).

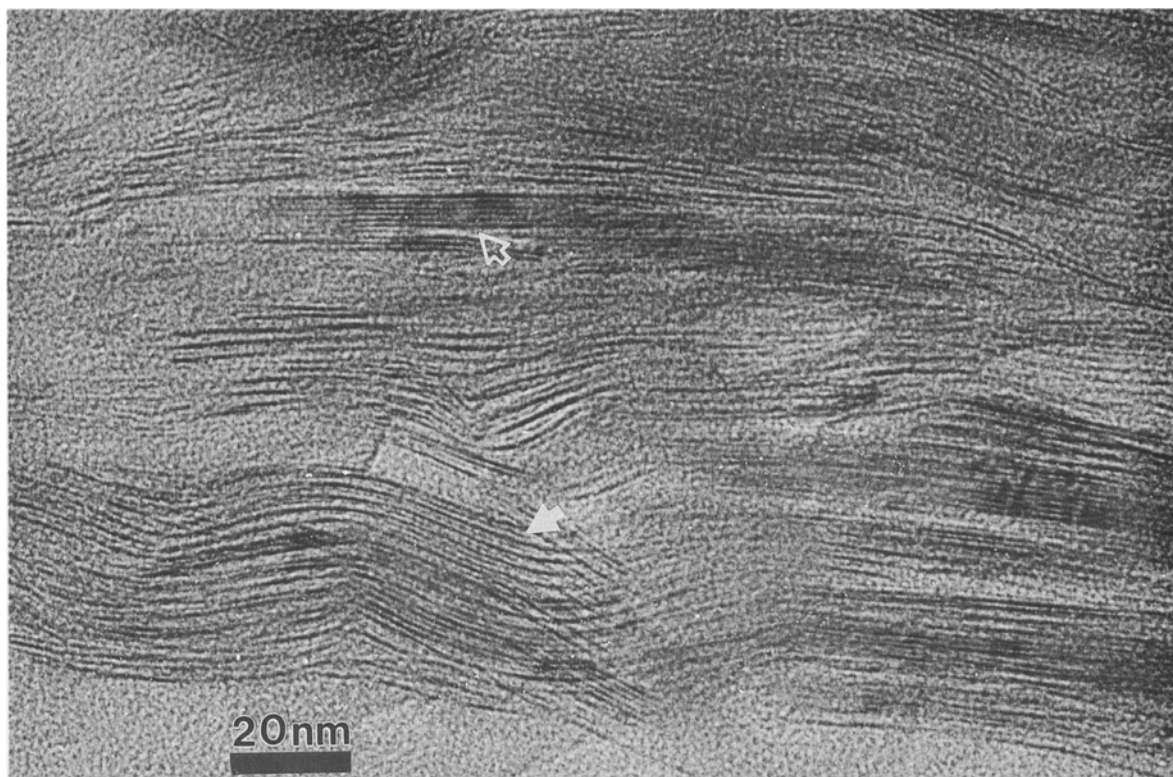


Figure 5. HRTEM lattice image of the C18-treated 0.02–0.06  $\mu\text{m}$  size fraction of the Webster soil showing two-layer elementary illite particles (solid arrow = 20.2  $\text{\AA}$ ) and multilayer illite (hollow arrow = 10  $\text{\AA}$ ).

monium treatment, however, did not achieve a stoichiometric exchange of octadecylammonium for Ca on the exchange complex of the clay. The C18-clay retained 1.75  $\text{g kg}^{-1}$  Ca (the Ca-saturated sample had 16.58  $\text{g kg}^{-1}$  Ca) after the C18-treatment.

X-ray diffraction patterns are presented in Figure 3 for a block of Quetol resin without clay (A), the C18-treated clay in a block of Quetol resin (B), and the C18-treated clay oriented on a glass slide (D). C in Figure 3 is a calculated XRD pattern obtained by subtracting A from B, and, hence, it represents the XRD pattern of the C18-treated clay in the epoxy resin without the resin effect. A comparison of patterns C and D indicates that embedding the C18-treated clay in epoxy resin caused little or no interlayer expansion.

Bright field lattice images taken by HRTEM (Figures 4 and 5) reveal three distinct types of mineral particles in the 0.02–0.06  $\mu\text{m}$  size fraction: 1) two-layer elementary illite particles, 2) one-layer elementary smectite particles, and 3) discrete multilayer illite particles. Kaolinite was not detected during HRTEM analysis of the 0.02–0.06  $\mu\text{m}$  size fraction, indicating that kaolinite contamination of the sample was minimal. The elementary illite particles were the most abundant particle type in this sample, with elementary smectite particles being the second most abundant particle type. Only a

few discrete multi-layer illite particles were observed (see hollow arrows, Figures 4 and 5). Estimates of the relative quantities of each particle type were not possible due to difficulties in resolving non-repeat spacings on the lattice images.

Figure 6 is a digitally enhanced (to improve contrast) enlargement of the lower right corner of Figure 5 showing a stack of subparallel elementary illite particles. The two-layer nature of elementary illite particles is readily apparent in Figure 6. Several stacking irregularities can also be observed in Figure 6, including what appears to be either random interstratification of one-layer elementary smectite particles between two-layer elementary illite particles or small segments of three-layer elementary illite particles (between arrows, Figure 6). Both the elementary illite particles and the elementary smectite particles commonly exhibited lattice curvature, suggesting that these particles are flexible. The discrete multi-layered illite particles, by contrast, did not exhibit lattice curvature.

The d-spacing of the elementary illite particles in Figure 6 is estimated to be 20.2  $\text{\AA}$ , substantially less than the 28  $\text{\AA}$  that was anticipated for an octadecylammonium-treated, two-layer, elementary illite particle (two 10  $\text{\AA}$  silicate layers plus one 8  $\text{\AA}$  octadecylammonium-saturated interlayer). This discrepancy is

thought to be an artifact of selective imaging. Sample orientation and degree of underfocus must be just right for images of irregular lattice spacings to be resolved (Ahn and Peacor, 1986). Consequently, high quality lattice images of stacks of elementary illite and smectite particles were observed in only a few locations on the sections, even though smaller lattice spacings [4.5 Å smectite (110), (1 $\bar{1}$ 0), and (020) lattice planes] could be readily observed in the same micrographs. Apparently, the stacks of elementary particles that were successfully imaged were those that retained interlayer Ca and hence exhibited more nearly regular spacing of 10.0 and 10.2 Å.

The existence of two-layer elementary illite particles was predicted by Laird *et al.* (1991a) solely from the chemistry of fine clay fractions (all <0.09  $\mu\text{m}$ ) separated from the Webster soil. Results presented in this study for HRTEM, XRD, and chemical analyses of the 0.02–0.06  $\mu\text{m}$  size fraction are consistent with the interpretations presented in the previous paper. Therefore, we conclude that 20 to 30% of the mass of the Webster soil clay (<2  $\mu\text{m}$  size fraction) consists of low-charge elementary illite particles. Calculations show that the low-charge illitic phase contributes nearly 25% of the total inorganic surface area and 25% of the cation exchange capacity for the Webster soil. Furthermore, the tendency of the low-charge illitic phase to collapse to 10 Å when K saturated and air-dried (C in Figure 2) suggests that the illitic phase has a large capacity to “fix” K.

Evidence for interstratification of illitic layers in soil smectites has been widely reported (Wilson, 1987; Sawhney, 1989); in the past, however, such layers have been considered an integral component of soil smectites. The results of this study and those of Laird *et al.* (1991a) demonstrate that the illitic phase in randomly interstratified smectite/illite from the Webster soil can be physically separated (or concentrated) from the smectitic phase and that the illitic phase has unique chemical, morphological, and mineralogical properties.

Classification of the low-charge illitic phase identified in this study is difficult. Conceptually and structurally, the low-charge illitic phase is similar to rectorite. Elementary particles from both rectorite and the low-charge illitic phase are composed of pairs of dioctahedral 2:1 phyllosilicate layers with alternate swelling and nonswelling interlayers; their charge characteristics, however, are substantially different. The non-swelling interlayers of rectorite contain about 0.85 univalent cations per formula unit and the swelling interlayers about 0.35 univalent cations per formula unit (Bailey *et al.*, 1982). In comparison, the elementary illite particles of the low-charge illitic phase have a nearly equal distribution of charge between the swelling and nonswelling interlayers (both about 0.47 per formula unit). On the other hand, under existing

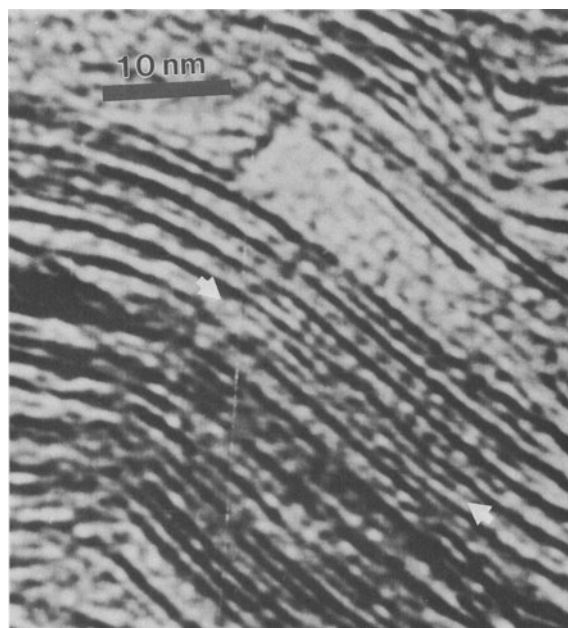


Figure 6. An enlargement of the lower left-hand corner (near solid arrow) of Figure 5 showing a stack of two-layer elementary illite particles. Digital image processing was used to enhance the contrast of this image. The individual layers of the two-layer elementary illite particles are clearly visible in this enlargement. Several stacking disorders are also visible, including a region (arrows) displaying what appears to be either a random interstratification of a single elementary smectite particle between two two-layer elementary illite particles or else a three-layer elementary illite particle.

nomenclature guidelines (Bailey *et al.*, 1982) a new mineral species name cannot be assigned to the low-charged illitic phase, because it does not exist in nature as a separate ordered entity but rather as a component of a randomly interstratified mineral. Clearly, the guidelines governing nomenclature need to be changed to facilitate discussion of elementary particles and irregularly interstratified minerals.

## REFERENCES

- Ahn, J. H. and Peacor, D. R. (1986) Transmission electron microscope data for rectorite: Implications for the origin and structure of “fundamental particles”: *Clays & Clay Minerals* **34**, 180–186.
- Bailey, S. W., Brindley, G. W., Kodama, H., and Martin, R. T. (1982) Report of the Clay Minerals Society Nomenclature Committee for 1980 and 1981: Nomenclature for regular interstratifications: *Clays & Clay Minerals* **30**, 76–78.
- Barak, P., Molina, J. A. E., Hadas, A., and Clapp, C. E. (1990) Optimization of an ecological model with the Marquardt algorithm: *Ecol. Modell.* **51**, 251–263.
- Bevington, P. R. (1969) *Data Reduction and Error Analysis for the Physical Sciences*: McGraw-Hill, New York, 336 pp.
- Jackson, M. L. (1985) *Soil Chemical Analysis—Advanced Course*: 2nd ed., M. L. Jackson, ed., Madison, Wisconsin, 100–166.

- Jackson, M. L., Lim, C. H., and Zelazny, L. W. (1986) Oxides, hydroxides, and aluminosilicates: in *Methods of Soil Analysis, Part 1: 2nd ed.*, A. Klute, ed., Soil Sci. Soc. Am., Madison, Wisconsin, 101–150.
- Kunze, G. W., and Dixon, J. B. (1986) Pretreatment for mineralogical analysis: in *Methods of Soil Analysis, Part 1: 2nd ed.*, A. Klute, ed., Soil Sci. Soc. Am., Madison, Wisconsin, 91–100.
- Laird, D. A., Scott, A. D., and Fenton, T. E. (1987) Interpretation of alkylammonium characterization of soil clays: *Soil Sci. Soc. Am. J.* **51**, 1659–1663.
- Laird, D. A., Thompson, M. L., and Scott, A. D. (1989) Technique for transmission electron microscopy and X-ray powder diffraction analyses of the same clay mineral specimen: *Clays & Clay Minerals* **37**, 280–282.
- Laird, D. A., Barak, P., Nater, E. A., and Dowdy, R. H. (1991a) Chemistry of smectitic and illitic phases in interstratified soil smectite: *Soil Sci. Soc. Am. J.* **55**, 1499–1504.
- Laird, D. A., Dowdy, R. H., and Munter, R. C. (1991b) Suspension nebulization analysis of clays by inductively coupled plasma-atomic emission spectroscopy: *Soil Sci. Soc. Am. J.* **55**, 274–278.
- Mackintosh, E. E. and Lewis, D. G. (1968) Displacement of potassium from micas by dodecylammonium chloride: *Trans. Int. Congr. Soil Sci.* **9th.** **2**, 695–703.
- Nadeau, P. H., Tait, J. M., McHardy, W. J., and Wilson, M. J. (1984a) Interstratified XRD characteristics of physical mixtures of elementary clay particles: *Clay Miner.* **19**, 67–76.
- Nadeau, P. H., Wilson, M. J., McHardy, W. J., and Tait, J. M. (1984b) Interstratified clays as fundamental particles: *Science* **225**, 923–925.
- Reynolds Jr., R. C. (1980) Interstratified clay minerals: in *Crystal Structures of Clay Minerals and their X-Ray Identification*, G. W. Brindley and G. Brown, eds., Mineralogical Society, London, 249–303.
- Sawhney, B. L. (1989) Interstratification in layer silicates: in *Minerals in Soil Environments: 2nd ed.*, J. B. Dixon and S. B. Weed, eds., *Soil Sci. Soc. Am.*, Madison, Wisconsin, 789–828.
- Theissen, A. A. and Harward, M. E. (1962) A paste method for preparation of slides for clay mineral identification by X-ray diffraction: *Soil Sci. Soc. Am. Proc.* **26**, 90–91.
- Wilson, M. J. (1987) Soil smectites and related interstratified minerals: Recent developments: in *Int. Clay Conf., Denver, Colorado, 1985*, L. G. Schultz *et al.*, eds., Clay Minerals Society, Bloomington, Indiana, 167–173.

(Received 7 December 1992; accepted 10 May 1993; Ms. 2299)